Lunds Universitets Institution för Naturgeografi och Ekosystemanalys

Seminarieuppsatser Nr. 92

Investigating the use of Landsat TM for mapping leaf nitrogen of Norway spruce

Stefan Lindquist

2002
Department of Physical Geography and Ecosystems Analysis,
Lund University
Sölvegatan 13, S-221 00 Lund,
Sweden

Abstract

Nitrogen in the green biomass of vegetation plays an important role in many biochemical processes in the terrestrial ecosystems, and often used as an input parameter to ecosystem models. It strongly influences photosynthetic rate, decomposition, and evaportanspiration, to name a few. Measuring nitrogen in field involves a lot of time and money, and it would be valuable if this part of the data collection could be done with remotely sensed data. In recent research, different methods has been used, statistical relationship, empirical/mathematical approaches or more sophisticated with the use of advance reflectance modeling, that all attempts to estimate or find a connection to nitrogen through remotely sensed data. Most of them have the thing in common that they use high-resolution reflectance data, so called hyper-spectral data.

In this study an investigation was done to find out how useful the spectral information from Landsat TM is, and if the reflectance values has any connection the needle nitrogen concentration of Norway spruce (*Picea abis* (L.) Karst.). Moreover, an evaluation of the PROSPECT model was done, both to find out the importance of each input parameter and to find out how they affect the reflectance. A fieldwork was carried out in the spring of 2000 where ten different Norway spruce stands in Scania were visited and various parameters measured, including the concentration of nitrogen in the needles.

No correlation was found between the reflectance data and nitrogen in the needles, the highest correlation coefficient was 0.48 (N.S). However, in a stepwise regression two TM channels were selected, TM1 and TM2, with an R^2-value of 0.72. This relationship, based on other studies, is assumed to origin from the correlation between nitrogen and chlorophyll and not the direct relation between reflectance and the needle nitrogen.

The evaluation of the PROSPECT model showed that nitrogen concentrations in leaves have little effect on the simulated reflectance. The biggest influence on the reflectance seems to be the active number of cell layers in the leaf and the leaves' chlorophyll concentration.

A gradient from west to east in the leaves nitrogen concentration was found, this with a regression analysis between easting coordinate (X) and nitrogen concentration (R^2 = 0.77). The gradient could not be observed in the remotely sensed data.

Sammafattning

Kvävekoncentrationen i den gröna biomassan hos vegetation är involverad i många olika biokemiska processer i det terrestra ekosystemet. Till exempel så påverkar den fotosyntesen, förmultning och evaportanspirationen, för att nämna några. Därför är den också ofta en av grundparametrarna och drivkraften i olika ekosystem-modeller. Att mäta kvävehalten hos blad/barr i fält kan vara både tidsödande och dyrt, varför det vore värdefullt att kunna uppskatta den med hjälp av fjärranalys. I olika studier har man använt: statistiska-, empiriska/matematiska metoder, eller lite mer sofistikerade reflektansmodeller. Alla vilka ämnar uppskatta eller hitta samband mellan reflektans och kvävekoncentrationen i löv. De flesta av studierna har den gemensamma nämnaren att de använt sig av hög upplösande reflektansdata, eller så kallad hyper-spektral data.

I denna studie har en undersökning utförts som utvärderar hur lämplig den spektrala information man kan tillhandahålla från Landsat TM är. Och ifall dess reflektansvärden har någon koppling till kvävehalten i barren hos gran (*Picea abis* (L.) Karst.). Utöver det har även en utvärdering av reflektansmodellen PROSPECT gjorts, både för att få veta vilka parametrar som är viktigast och för att se hur de påverkar den modellerade reflektansen. Ett fältarbeta utfördes på våren år 2000 där tio stycken granskogsbestånd besöktes i fält. Olika beståndsparametrar mättes, däribland kvävehalten hos barren.

Ingen korrelation kunde fastställas mellan reflektansdatan och kvävehalten i barren, den högsta korrelations koefficienten var 0.48 (N.S). Däremot så gjordes även en *stepwise regression* där två TM kanaler valdes ut, TM1 och TM2, detta med ett R^2-värde på 0.72. Detta samband, baserat på andra studier, anses komma från korrelation mellan kväve och klorofyll och inte det direkta förhållandet mellan reflektans och kväve i barren.

Utvärderingen av PROSPECT modellen visade att kvävehalten hade väldigt litet inflytande på den simulerade reflektansen. Det största inflytande hade antalet aktiva cellager i lövet och dess klorofyllkoncentration.

En gradient från väster till öster i bladets kvävehalt har upptäckts, detta med hjälp av regressionsanalys mellan X-koordinat och kväve koncentration (R^2 = 0.77). Gradienten kunde inte observeras i fjärranalys datan.

Acknowledgement

This paper is the result of the final examination in the Physical Geography Programme, Department of Physical Geography and Ecosystems Analysis, Lund University, Sweden. I want to express a special thanks to my supervisor PhD Lars Eklundh, who has been of invaluable help, guiding and helping me out with ideas. I also wish to thank the following people who have provided me with data or helped me out with guidance or ideas:

Gunnar Thelin	Section of Plant Ecology, Department of Ecology, Lund University.
Johan Holmqvist	Center for Chemistry and Chemical Engineering, Lund Institute of Technology, Lund University.
Patrik Wallman	Center for Chemistry and Chemical Engineering, Lund Institute of Technology, Lund University.
Andres Kuusk	Tartu Observatory, Estonia.
Thomas Person	Research and Development, SMHI.

Contact information:

Stefan Lindquist
Kämnersvägen 13F104
226 46 Lund
Stefan.Lindqvist.988@student.lu.se

Lars Eklundh (supervisor)
Dept. Physical Geography and Ecosystems Analysis
Lund University
Box 118, 221 00 Lund
Lars.Eklundh@nateko.lu.se

Table of Contents

1. Introduction

Many of the biogeochemical processes, such as photosynthesis, net primary production, evapotranspiration, and decomposition are related to the content of chlorophyll, nitrogen, water, lignin, and cellulose in leaves (Dawson *et al*., 1999; Jacquemoud *et al*., 1996). For example, a single leaf with high photosynthetic rate has high biochemical concentration, such as chlorophyll or nitrogen concentration (Endo *et al*., 2000). The different biochemical concentrations and the processes are used in models of forest ecosystems (Curran *et al*., 2001), for yield prediction in agricultural systems, (Hosgood *et al*., 1995) for estimation of vegetation stress, and to identifying tree species (O'Neill *et al*., 2002). By using remote sensing to estimate the concentrations of the biochemical contents in the leaves, one would be able to collect data over a wider ranger, both faster and eventually cheaper then a normal data collection through fieldwork (Serrano *et al*., 2002; Kokaly & Clark, 1999).

In recent research, different methods have been used for estimating nitrogen (surrogate of protein (Jacquemoud *et al*., 1996)), or other biochemical constituents, often with the use of a hyper-spectral data, like the data from AVIRIS sensor (Airborne Visible / Infrared Imaging Spectrometer). Nitrogen data (and/or other biochemical constituent) are collected in the field and processed together with hyper-spectral data, for example with the use of multiple stepwise regressions. Kokaly and Clark (1999) received good results correlating biochemical data from dried leaves and reflectance data gathered with a hyper-spectral sensor. For the investigation of reflectance properties of leaves with different biochemical composition, theoretical models are useful. One example of such a model is PROSPECT by Jacquemoud & Baret (1990) and Jacquemoud *et al*. (1996).

1.1. Aim

The aim with this study is to investigate how nitrogen in the needles of Norway spruce (*Picea abis* (L.) Karst) influences the canopy reflectance observed with Landsat 5 Thematic Mapper (TM). Partial goals were formulated:

- To obtain correct reflectance values at ground level through an atmospheric correction scheme
- To investigate the theoretical response of the reflectance, due to nitrogen concentration, with use of a radiative transfer model
- To find statistical relationship between various field data and the reflectance measured with remotely sensed data.

1.2 Chapter summary

This summary aims to give the reader a brief outline of the different chapters in this essay. Chapter 2 contains the theoretical background concerning leaves, leaf reflectance, and canopy reflectance. Chapter 3 describes some of the methods used when trying to estimate the biochemical concentrations from leaves using remotely sensed data. The different processes to archive a correct satellite image is described in chapter 4. Chapters 5, 6, and 7 contain methods, results, and discussion from this study respectively.

2. Leaf structure

To understand spectral properties of vegetation, knowledge of the internal structure of individual leaves is needed. In Figure 1, a cross section of a typical leaf is demonstrated. The upper layer of the leaf, called upper epidermis, is made up of specialized cells arranged so that no gaps or openings exist. On the surface of these cells there is a wax layer called cuticule, which prevents moisture loss from within the leaf. A similar layer as the upper epidermis exists on the underside of the leaf, called lower epidermis. The only difference is the stomates, and the two guard cells on each stomata, that control the gaseous transport to and from the leaf and to regulate the leaf's temperature. Below the upper epidermis is a layer called palisade tissue that is build up by vertically elongated cells. Palisade cells include chloroplasts, which are cells composed of chlorophyll and other pigments that are active in the photosynthesis. Under the palisade tissue, there is a layer of spongy mesophyll tissue, with irregular shaped cells separated by interconnected openings. Here processes involving carbon dioxide and oxygen exchange occur, which is necessary for photosynthesis and respiration (Campbell, 1996).

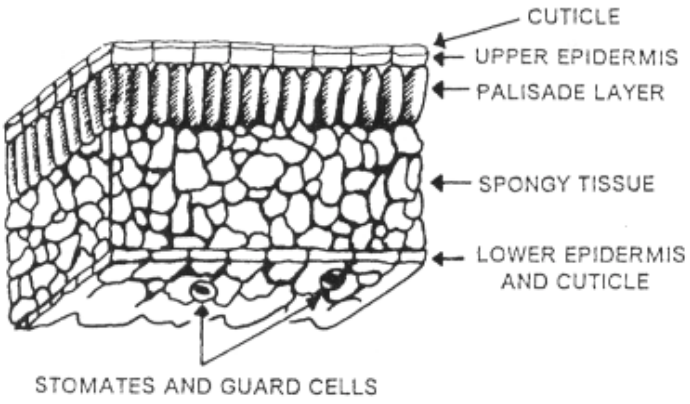

Figure 1. A cross section of a typical leaf (Campbell, 1996).

2.1. Spectral behavior of a leaf

The spectral response of a leaf is mainly controlled by the photosynthetic pigments (chlorophyll a, chlorophyll b and carotenoids) in the visible part (400-700 nm) of the spectrum (Danson, 1995). The pigments absorb both blue and red light for use in the photosynthesis, while somewhat more of the green light is reflected. Eventually 70-90% of the incoming radiation in blue and red wavelengths is absorbed (Campbell, 1996). The internal structure of a leaf is the cause of the near infrared (700-1300 nm) reflectance of living vegetation (Campbell, 1996), especially the arrangements and the number of air spaces between the cells are important (Danson, 1995). Both the epidermis and the cuticle are very transparent to infrared radiation and the majority of the radiation is transmitted to the spongy mesophyll tissue. The spongy mesophyll tissue scatters the infrared radiation both upward and downward and only a fraction is absorbed (Campbell, 1996). In some regions, both in near infrared and middle infrared (1300-3000 nm), the reflectance is affected by leaf water content. The water absorption bands are located at approximately 1950, 1450, 1175 and 970 nm. Absorption also occurs in different wavelengths by other biochemical constituents in leaves such as protein, lignin and cellulose (Danson, 1995). Nitrogen has been reported to have several different absorption features throughout the spectrum; most of them are located in the infrared- and middle infrared wavelengths. Curran & Kupiec (1995) suggests 1020, 910 and 2350 nm and Wessman 1510, 1980, 2060, 2180 and 2300 nm as the main absorption wavelength's for nitrogen/protein.

2.2. Canopy reflectance

To explain the spectral characteristics of a canopy not only information of the leaves' spectral behavior is needed, but also about several other factors. The canopy consists of many individual trees; each tree has a set of branches and each branch a set of leaves. The leaves may differ in size, orientation and shape, creating, together with the ground, shadowing and the structural variables as stems and branches, a complex structure of elements that influence the canopy reflectance as whole. The shadowing from the upper

leaves decreases the overall reflectance of the canopy, but the reduction is not uniform over the spectrum. In a canopy, the decrease of reflectance may be as high as 70 % in the visible part of the spectrum while only 30% in the near infrared part, compared to a single leaf. This as the incoming radiation has to travel through the canopy and the visible part is affected by chlorophyll absorption while the leaves transmit or reflect the radiation in near infrared to a higher grade (Campbell, 1996).

Danson (1995) describes the most important factors affecting the canopy reflectance as:

- Leaf area index (LAI), the area leaf over an area ground (m^2/m^2)
- Leaf optical properties – reflectance, transmittance and absorptance
- Leaf location in three-dimensional space - vertical and horizontal distribution of leaves and degree of 'clumping'
- Leaf orientation in three-dimensional space – leaf inclination angle distribution and leaf azimuth angle distribution
- Reflectance of the understorey vegetation, soil or other background
- Geometry of illumination and view.

One important variable not mentioned above is canopy cover. Generally, in agricultural crops, the LAI and canopy cover are closely related, but in a forest, these variables may differ substantially. The canopy cover controls the amount of understorey vegetation or soil that is visible from above (Danson, 1995).

Other stand variables such as stand density, age, tree height and basal area may be correlated to the canopy reflectance. However, they are often regarded to have a non-casual relationship as they usually are closely related to LAI or canopy cover (Danson, 1995).

3. Estimation of leaf biochemical parameters from reflectance

3.1. Mathematical approach

The mathematical approach to determine leaf biochemical constituents involves several different methods. One method, called spectral mixture analysis, compresses the spectral information $\rho(\lambda)$ of a complex target into independent sources of variability, the end-members (Jacquemoud, 1993). At leaf level, one considers the specific absorption coefficients $k_i(\lambda)$ of chlorophyll, water, protein, cellulose, lignin, and more as end-members and the coefficients C_i are the concentrations to retrieve. The concentrations of C_i are the values that produce the best fit of $\rho(\lambda)$ (Jacquemoud & Ustin, 2001). For further description of the technique, Goetz *et al.* (1990) is recommended.

Another technique that is frequently used is multiple stepwise regression (Zar, 1996). Here, a direct regression equation is established between leaf reflectance (or transmittance or absorptance) at a few wavelengths $\rho(\lambda_i)$, and the biochemical content of one of its constituents C. The wavelengths selected by the procedure are those that minimize the RMSE (Root Mean Square Error) of the regression. This method requires data for both establish the regressions (calibration set) and a data set (validation set) to validate them (Jacquemoud & Ustin, 2001). Curran and Kupiec (1995) published good results using this technique when relating high-resolution reflectance data from a forest canopy and different concentrations of foliar biochemical's.

Neural network is another method that has shown potential to estimate biochemical parameters in a leaf (Jacquemoud & Ustin, 2001). The algorithms, caricature the way information is processed in biological networks of neurons. They are defined mainly by the type of neuron used, the way they are organized and connected (the network architecture) and the learning rule. Neural networks have been recognized as a very powerful tool to discriminate between variables or to relate one set of variables to another (Baret, 1995).

3.2. Modeling the canopy reflectance

With use of models, one tries to simulate the interaction between solar radiation and the different vegetation elements. The models are built by the known processes, incorporate the information into a model, which relates the vegetation characteristics and spectral properties (as reflectance or spectral signatures). As described in chapter 2.2 the reflectance of a canopy depends on the canopy characteristics or a set of parameters, here *C*, wavelength (λ), the direction of the incident solar radiation, and the view direction (Goel, 1989). This can be described symbolically by:

$$S = R(t; \lambda; \theta_s; \psi_s; \theta_o; \psi_o; C) \quad (1)$$

where:

S = spectral signature or reflectance of the canopy

t = the emergence time of the plant (temporal change in the vegetative spectral signature)

λ = wavelength of the incident solar radiation

θ_s and ψ_s = solar zenith and azimuth angles, respectively

θ_o and ψ_o = view zenith and azimuth angles, respectively

C = canopy parameter (s)

R = the functional dependence of S on these parameters

However, the value of C is the one to determine from the remotely sensed data (S) and the equation (Eq. 1) represents the direct approach, thus the equation need to be inverted. This is done by finding the merit function F that best represent the inversion of the model. The process to find F is usually complicated mathematically and may take a lot of computation time (Goel, 1989).

3.2.1 PROSPECT and other leaf optical models

Sometimes a sub-model is included in canopy reflectance models that model the leaf optical properties. The simplest leaf optical models simulate the leaf as a single scattering

and absorbing layer. While the most advanced describes the cells in detail with parameters like shape, size, position, and biochemical content (Jacquemoud & Ustin, 2001). Leaf optical models can be separated into four different types (Fig. 2a-d):

- Plate models (Fig. 2a), which represent the leaf as one or several absorbing plates with rough surfaces giving rise to isotropic diffusion
- N-flux models (Fig. 2b), which considers the leaf as a slab of diffusing and absorbing material
- Stochastic and other radiative transfer models (Fig. 2c), where the leaf is partitioned into different tissues and its optical properties is simulated by a Markov chain, or eventually based on the radiative transfer equation
- Ray tracing models (Fig. 2d), that require a detailed description of the internal leaf structure and the optical constants of leaf material

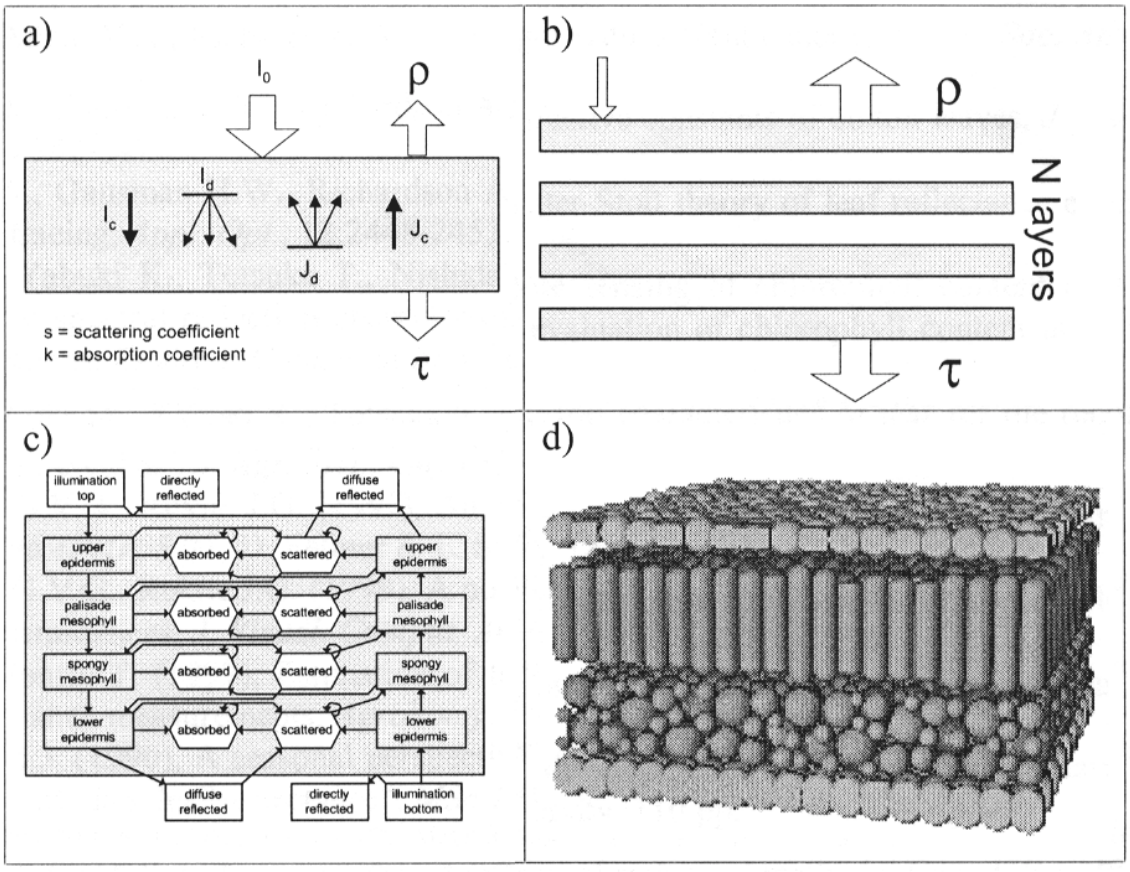

Figure 2. Schematic description of different leaf optical models, a) Plate model, b) N-flux model, c) Stochastic and radiative transfer model, and d) Ray tracing model (Jacquemoud & Ustin, 2001).

The PROSPECT model (Jacquemoud & Baret, 1990; Jacquemoud *et al*., 1996) is an example of a leaf optical model based upon the plate model in Figure 2a. This radiative transfer model calculates the leaf hemispherical reflectance and transmittance in the wavelengths 400 nm to 2500 nm. In the early version (Jacquemoud & Baret, 1990), the input parameters were: *N* – the parameter that characterizing the leaf mesophyll structure, *Cab* – chlorophyll (a+b) concentration and *Cw* – water depth. Later the model was pre-defined (Jacquemoud *et al*., 1996) to include other biochemical constituents, *Cp* – protein concentration and *Cc* – lignin and cellulose concentration. The model is invertible and has been successfully incorporated in canopy reflectance models as LIBERTY (Dawson *et al*., 1998), Forest reflectance model (Kuusk & Nilson, 2000) and SAIL (Jacquemoud, 1993).

4. Preprocessing of a satellite image

4.1. Radiometric and atmospheric correction of satellite data

The purpose with a radiometric correction is to convert the DN-values (digital numbers) to absolute radiance values. Absolute radiance is required when utilizing temporal data that may come from different sensors (normalize) or when using radiation as input to mathematical/physical models. The relation between acquired DN-values and the radiation is usually linear, an example of this linear relationship for Landsat-TM can be seen in Figure 3a. It can also be described with the formula (Lillesand & Kiefer, 2000):

$$DN = G * L + B \tag{2}$$

where

DN = digital number

G = channel gain

L = spectral radiation measured

B = channel offset

By inversion of the radiometric response (Fig. 3b) the radiance may be calculated with:

$$L = \left(\frac{L\max_i + L\min_i}{DN\max} \right) DN + L\min_i \qquad (3)$$

where

L = spectral radiance

DN = digital number

DNmax = max value a DN can have

$Lmin_i$ = radiance at DN-value 0, channel i

$Lmax_i$ = radiance at max DN-value, channel i

Lmax and Lmin are known values for a specific sensor and the radiance unit is expressed as mW/cm^2 sr μm (Lillesand & Kiefer, 2000).

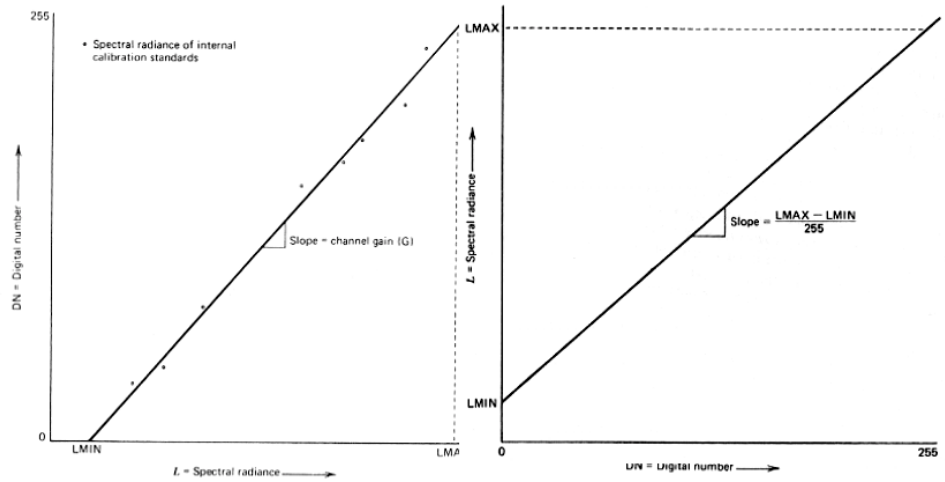

Figure 3. The linear relationship between Landsat TM's DN-values and radiation, a) normal relationship, and b) inverted relationship (Lillesand & Kiefer, 2000).

Another part of the radiometric correction is to calculate at-satellite reflectance from the radiance values. This operation corrects for different sun-zenith angels and a seasonal change in the earth-sun distance. At-satellite reflectance can be calculated with (Markham & Baker, 1986):

$$pp\lambda = \frac{\pi L_i d^2}{Esun_i \cos(v)} \quad (4)$$

where

$pp\lambda$ = Unit less effective at-satellite reflectance

L_i = Spectral radiance (mW/cm^2 sr μm) from Equation 3

d = Earth-sun distance in astronomical units

$Esun_i$ = Mean solar exoatmospheric spectral irradiance in $mW/(cm^2$ μm)

V = Solar zenith angle in degrees

4.1.1 Atmospheric effects and its correction

The atmosphere can influence the direct solar radiation and the radiation reflected back by targets on earth's surface, thus changing the signal received by a satellite sensor (Kaufmann, 1989). The photons can be lost because of two processes: absorption and scattering. Only a fraction of the photons coming from the target reaches the satellite sensor, 80% at 0.85μm and 50% at 0.45μm. This makes the target look less reflecting (Vermote, 1997a).

Vermote (1997a) describes the different processes how the photons are scattered by the atmosphere on the Sun-surface and surface-satellite path:

- Some of the photons, traveling from the sun towards earth, will not reach the surface and are backscattered toward space. As this signal never reach the earth it will be independent of the surface reflectance and have the same value for a uniform, non-uniform, or non-Lambertian surfaces. It will only be a term of interference and may cause a loss of contrast in the image (Vermote, 1997a; Kaufman, 1989).

- The remaining photons contribute to the illumination of the ground by the way of scattering paths and compensate the attenuation of the direct solar paths. This diffuse component has therefore to be considered in the useful signal.

- By the same way, a fraction will be scattered toward the sensor, making photons not inside the sensors field of view to be received by the satellite. If the surface is uniform, it is a useful component but if the surface has a patchy structure, this term will introduce environment effects that will be a perturbation.

- A fraction of the photons reflected by the surface will be backscattered by the atmosphere to the surface. This creates a third component of its illumination called the trapping effect.

As the atmosphere has its own signature, it is important to correct for this when trying to derivate biochemical parameters at canopy level or when the signal is used in canopy reflectance models (Baret, 1995). There are different approaches to do the absolute calibration of the satellite reflectance, some more sophisticated then others. Some of methods are: histogram minimum method (HMM), covariance matrix method (CMM) and physical models (Campbell, 1996). Most widely used physical models are LOWTRAN (Kniezys *et al*., 1988), MODTRAN (Berk *et al*., 1989) and 6S (Vermote, 1997a; Vermote, 1997b).

4.2. Geometric correction

Geometric errors often occur in remotely sensed images. The distortions may come from variations in altitude, attitude and velocity of the sensor platform. When studying different objects in a satellite scene it is desired to have the coordinates as correct as possible. To correct for these errors, ground control points (GCP's) are collected and analyzed. GCP's represent objects of known location in both the geometric correct map (or GPS-points) and the distorted image, road intersections and distinct shorelines make good points. The GCP's, which includes information of the distorted image coordinates (row, column) and reference map coordinates (x-, y-values), are used in a least square regression analysis. The outcome of the analysis is functions to interrelate the uncorrected image to the geometric correct coordinates (Lillesand & Kiefer, 2000).

Example:

$$x = f_1(X, Y)$$
$$y = f_2(X, Y) \quad (5)$$

where

(x, y) = distorted-image coordinates (column, row)

(X, Y) = correct (map) coordinates

f_1, f_2 = transformation functions

The transformation functions (f_1, f_2) may be polynoms of different orders, 1st to 5th. Generally, the higher the order of the polynomial transformation, the better accurate fit in the near surrounding area of the GCP's. However, away from the GCP's, worse errors may be introduced into the image than were to be corrected (GCPWorks, reference manual 6.2, 1997).

A part of the correction scheme is to resolve the new pixel values from the uncorrected image to the corrected image, resampling. There are different methods for resampling: Nearest neighbor technique being the simplest, by letting the new pixel DN represent the closest pixel's DN from the original image. Bilinear interpolation calculates the new values based on distance-weighted average of the DN's from the four closest pixels. In addition, cubic convolusion method, where the new pixels values are resolved by evaluation of the block of 16 pixels in the uncorrected image that surrounds each pixel in the new image. Nearest neighbor have the advantage with no pixels value being altered while both bilinear interpolation and cubic convolusion alter the original pixel values (Lillesand & Kiefer, 2000).

5. Methods

5.1. Data and instruments

The instruments used in this study were:

- A Magellan hand-held DGPS was used to get the coordinates for the different stands. Approximate precision is ~5m
- An inclinometer was used to obtain tree height and crown inception (latter used to obtain crown height)
- A diameter-tape measure was used to get a tree's breast height diameter
- A 'mirror crown-radius measure' was used to obtain a tree's crown radius.

The data used in this study were:

- Atmospheric data (7 April, 2000) from Thomas Person was used in the atmospheric correction scheme
- Destructive measurements of different needle distribution in a Norway spruce tree (Gunnar Thelin, personal communication). This was used to calculate the percent distribution of different needle-ages.
- A Landsat 5 TM scene (194/21 7 April 2000) was used to obtain reflectance values from the different stands
- Rasterized topographic map (Gröna kartan) was used in the geometric correction scheme.

5.2. The stands and the fieldwork

In the last fifteen to twenty years, a project that aims to investigate forest detriment has established permanent study sites in Sweden (Skånes Samrådsgrupp mot Skogsskador, 1986; 1987; 1992a; 1992b; 1993 and 1997). Most of these stands are of coniferous type but a few deciduous stands also exist. All the coniferous stands were visited in field, but only ten Norway spruce stands were selected for this study (Fig. 4 and Tab. 1). They were selected on the basis:

- It had to be a Norway spruce stand (not Scots pine)
- The stand had to be homogenous and represent at least 90m X 90m (the same as 3 X 3 pixels in a Landsat TM scene)
- Some of the Norway spruce stands were affected by the autumn storm –99, the stand should not have visual effects from this.

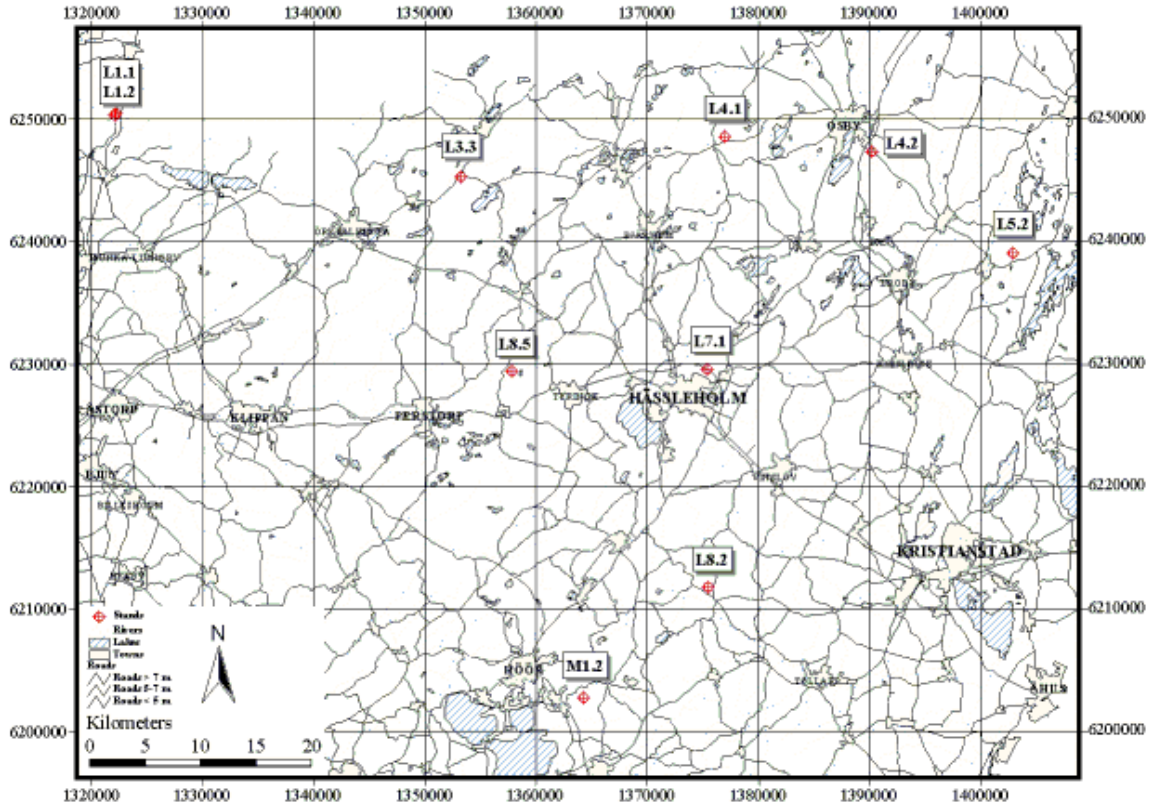

Figure 4. Map of the stands in central Scania, Sweden. The specific coordinates, size and age is shown in Table 1.

Table 1. The selected stands used in the study. X- and Y-coordinates are in reference system RT90.

Stand ID	Northing (Y)	Easting (X)	Size (m^2)	Age (2000)
L1.1	6252648	1322168	400	39
L1.2	6252830	1322232	400	54
L3.3	6247120	1353340	400	49
L4.1	6250790	1377070	600	59
L4.2	6249454	1390274	800	54
L5.2	6240274	1402956	400	39
L7.1	6229940	1375526	900	49
L8.2	6210300	1375570	400	39
L8.5	6229706	1357944	400	54
M1.2	6200360	1364375	900	69

The fieldwork took place in March to April 2000, and various stand parameters were collected. Breast-height diameter (DBH, denoted *d*) was taken from all trees in the area of interest (defined permanent study site). The height (*h*) and crown length (*kl*) of the trees were measured with an inclinometer, this on a sample of ten trees in each stand. On five trees, crown radius (*cr*) was measured using 'mirror crown-radius instrument'. The measurement was done on five different spots around the tree to adjust for irregular tree crowns. Five GPS-points were taken in each of the ten stands, one for each corner and one in the middle of the stand. The GPS-points were measured with an average of three minutes, and then a center value of the stand was calculated. Moreover, a sample of needles was taken from the top of five trees in each stand, to be measured in laboratory and to extract nitrogen concentrations. The amount of nitrogen in the needles was extracted using Kjelldahl's method (Balsberg-Phålson, 1990). The needles were not only from the current year shoots, but also from one, two and three years back (denoted as *C*, *C*+1, *C*+2 and *C*+3, where *C* is year 2000, *C*+1 is year 1999 etc.). A weighted average of the nitrogen amount (*wc*) was calculated from needle distribution data from Gunnar Thelin (personal communication).

LAI was calculated using a method described in Nilson *et al*. (1999). The method relates the tree's needle-biomass (Eq. 6) with a conversion factor for the needles weight per area (one-sided needle area). The needle biomass were calculated using one of Marklund (1988) regressions for biomass in spruce:

$$\ln(M) = -1.5732 + 8.4127\frac{d}{d+12} - 1.5628\ln(h) + 1.4032\ln(kl) \quad (6)$$

where

M = Needle biomass (kg)

d = Breast-height diameter (cm)

h = Tree height (m)

kl = Crown length (m)

The LAI values were calculated using the specific leaf weight of 152 g/m^2 (Nilson *et al*., 1999).

5.3 Landsat TM processing

5.3.1 Pre-processing

Both a geometric- and a radiometric correction were performed on the Landsat TM scene. The geometric correction was performed in GCPWorks (GCPWorks, reference manual 6.2, 1997) and with the use of rasterized Gröna kartan. A set of 58 GCP's were collected from different parts of Scania and applied to the image with use of 3rd grade polynoms and nearest neighbor resampling technique. At this stage, 3 x 3 pixel-values of each stand were extracted from the center of each stand using the GPS points collected in field. A radiometric correction was perform on the DN-values using Equations 3 and 4 and the values in Table 2. To be noticed, the values of Lmin and Lmax for each TM-channel are new correction values from the satellite manufacture as the sensor has gone through a smaller degradation over the years (ESA, 2002).

Table 2. Values used in the radiometric correction scheme. Unit of Lmin, Lmax and Esun is mW/cm^2 sr µm. NIR is the short for near infrared and MIR short for middle infrared. The wavelength is in the unit µm.

TM-channel	**TM 1**	**TM 2**	**TM 3**	**TM 4**	**TM 5**	**TM 7**	**Source**
Part of spectrum	Blue	Green	Red	NIR	MIR	MIR	
Wavelength	0.45-0.52	0.52-0.60	0.63-0.69	0.76-0.90	1.55-1.75	2.08-2.35	
Lmin	-0.15	-0.31	-0.27	-0.25	-0.045	-0.03	ESA (2002)
Lmax	18.5	34.2	24.5	27	3.6	1.9	ESA (2002)
Esun	195.7	182.9	155.7	104.7	21.93	7.452	Markham & Baker (1986)

5.3.2 Atmospheric correction with 6S-model

6S stands for "Second simulation of the Satellite Signal in the Solar Spectrum", and is a model that modulates the atmospheric effects on satellite signal from various atmospheric properties. For a thorough description of the model and input parameters, see Vermote *et al.* (1997a) and Vermote *et al.* (1997b).

The atmospheric conditions were described with the help of data received from Swedish Meteorological and Hydrological Institute, measured the same day and time as the satellite scene. The data included water vapor, ozone value and a β-value (Ångström's turbidity factor) that is used to calculate the atmospheric optical thickness at 550 nm ($\tau^A(550)$) (Kuusk, 1994). A maritime aerosol model was used to describe the aerosol conditions in the atmosphere as no data of aerosol content could be obtained, this is a pre-defined sub-model in 6S. The ground type was set to homogenous and vegetated with use of no directional model. An example of an input file can be seen in Appendix 1. The value of the atmospheric corrected reflectance was calculated for each Landsat TM-channel and for each stand, an example of the output can be seen in Appendix 2.

5.3.3 Spectral indices

To further extend the satellite data analysis different indices were introduced. These are well described and have been used before with success. The indices are shown in Table 3.

Table 3. The indices created from the different TM-channels.

Index	**Equation**	**Reference**
SR	TM4 / TM3	Jordan (1969)
MSI	TM5 / TM4	Vogelmann (1990)
NDVI	(TM4-TM3) / (TM4+TM3)	Rouse *et al*. (1974)
NDVI4:7	(TM4-TM7) / (TM4+TM7)	Nemani *et al*. (1993)

5.4. Reflectance modeling with the PROSPECT-model

A sensitivity analysis was performed on the PROSPECT-model (chapter 3.2.1.). The idea of the sensitivity analysis is to investigate how much each input parameter (*N*, *Cab*, *Cw*, *Cp* and *Cc*) of the model contributes to the output, in this case reflectance values. Each input parameter has a base value, which was obtained from e-mail correspondence with Andres Kuusk. These values are only theoretical and has no connection to the stands investigated in this study. Modeling is executed on one input parameter at a time, from continues series of -30%, -20%, -10%, ±0%,…, +30% of the base value, while the rest of the parameters are kept fixed to their base value. The result of this is a set of reflectance data that correspond to the continues change in that input parameter. This is done for all input parameter, creating a set of reflectance data for each input parameter that can be visually viewed and analyzed. The different values, including the base values that were used in the sensitivity analysis is shown in Table 4.

Table 4. The values of the different PROSPECT-parameters used in the sensitivity analysis. N is number of cell-layers, Cab is chlorophyll (a+b) in µg/cm^2, Cw is water thickness in cm, Cp is protein in g/cm^2 and Cc is cellulose and lignin concentration in g/cm^2.

Percent	N	Cab	Cw	Cp	Cc
-30	1.11342	49	0.025571	0.00014	0.00133
-20	1.27248	56	0.029224	0.00016	0.00152
-10	1.43154	63	0.032877	0.00018	0.00171
0	1.5906	70	0.03653	0.0002	0.0019
10	1.74966	77	0.040183	0.00022	0.00209
20	1.90872	84	0.043836	0.00024	0.00228
30	2.06778	91	0.047489	0.00026	0.00247

To better understand what impact each parameter had on the reflectance, a dimensionless index of sensibility (β) was used (slightly modified from: Friend, 1995):

$$\beta = \left| \frac{x_1 - x_0}{x_0} / \frac{p_1 - p_0}{p_0} \right| \qquad (7)$$

where:

β = dimensionless index of sensibility

x_1 = simulated value of the reflectance for parameter p_1

x_0 = simulated value of the reflectance for parameter p_0

p_1 = parameter that represent the reflectance in x_1 (e.g. 30% change)

p_0 = parameter that represent the reflectance value in x_0 (base value)

The β-value was calculated for each parameters base value versus the value that represents a +30% change in same parameter. To archive comparable data, the median value of the reflectance (simulated) in the wavelength-boundaries for each Landsat TM-channel were used (see Table 2 for the different wavelength-boundaries).

5.5. Statistical analysis

The statistical part of the study focused on investigating connections between the nitrogen values and the reflectance or eventually another stand parameter. A correlation

analysis was performed on the data set to search out possible relationship between the data. A stepwise regression was performed on the weighted average of nitrogen with all the Landsat TM-channels as possible predictors. Method used to eliminate predictors was ‘backward selection’ with an alpha-value set to 0.05. The different stands were also classified into two classes (straight cut), high- and low nitrogen status. These were plotted against the different TM-channels to eventually find indication of separabillity in their spectral data. Based on the correlation results, a regression analysis was performed for the weighted average of nitrogen and the stands’ X-coordinate.

6. Results

6.1. Stand parameters and LAI-calculation

The result from the fieldwork and the LAI-calculation is illustrated in Table 5. The table also includes standard deviation and the average for all the stands.

Table 5. The different stand parameters measured in the field. SD = stand density, d = breast height diameter (m), h = tree height (m), kl = crown length (m), cr = crown radius (m), c, c+1, c+2 and c+3 = nitrogen amount for each year respectively (mg/g), wc = weighted average of nitrogen (mg/g) and LAI = leaf area index.

Stand ID	SD	d	h	kl	cr	c	c+1	c+2	c+3	wc	LAI
L1.1	0.08	26.42	20.67	9.63	2.04	15.33	14.62	14.01	12.87	13.92	7.50
L1.2	0.10	24.84	21.86	9.23	1.54	15.75	14.66	13.79	12.69	14.03	6.86
L3.3	0.07	25.75	20.67	10.29	1.78	13.32	12.91	11.82	10.89	12.07	6.39
L4.1	0.08	21.91	22.65	11.70	1.70	11.90	11.51	10.46	10.81	10.85	6.28
L4.2	0.06	23.61	23.20	9.75	1.53	10.12	10.07	10.05	9.36	9.55	3.96
L5.2	0.08	20.75	18.50	9.05	1.54	11.44	10.98	10.89	10.03	10.53	5.35
L7.1	0.11	23.75	22.35	9.20	1.33	12.02	10.92	10.62	9.27	10.61	6.96
L8.2	0.14	20.17	19.14	8.18	1.20	14.09	13.03	12.10	11.89	12.53	7.19
L8.5	0.08	22.40	19.17	8.71	1.49	13.02	11.44	10.25	10.35	11.15	5.39
M1.2	0.05	34.67	26.33	10.08	2.00	11.86	12.06	11.78	10.95	11.27	5.33
Average	0.08	24.43	21.45	9.58	1.61	12.88	12.22	11.58	10.91	11.65	6.12
Std	0.03	4.14	2.35	0.97	0.27	1.78	1.56	1.41	1.25	1.47	1.10

6.2. Correction of the satellite image

The radiometric and atmospheric correction resulted in a linear equation that converts the DN-value to the correct reflectance at ground level for each TM-channel. These are presented in Table 6. The geometric correction resulted in a RMSE of 0.21 in the X-coordinate and 0.17 in the Y-coordinate using 3rd grade polynom.

Table 6. The equations used to convert from DN-value (DN_i) to an atmospheric corrected reflectance (R_i) where i = channel. R^2 = 1 for all the equations.

Channel	Equation
TM1	$R_1 = - 0.106 + 0.00257\ DN_1$
TM2	$R_2 = - 0.0578 + 0.00471\ DN_2$
TM3	$R_3 = - 0.0363 + 0.00368\ DN_3$
TM4	$R_4 = - 0.0246 + 0.00565\ DN_4$
TM5	$R_5 = - 0.0130 + 0.00277\ DN_5$
TM7	$R_7 = - 0.0250 + 0.00584\ DN_7$

6.3. Sensitivity of PROSPECT

The sensitivity analysis resulted in a set of reflectance values for each parameter that had been changed gradually. These values were then plotted versus the wavelength creating diagrams that is shown in Figures 5a-5e.

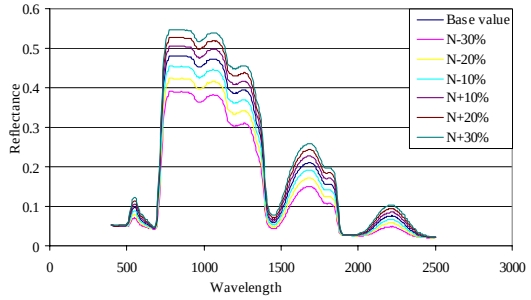

a) Cell layers (N)

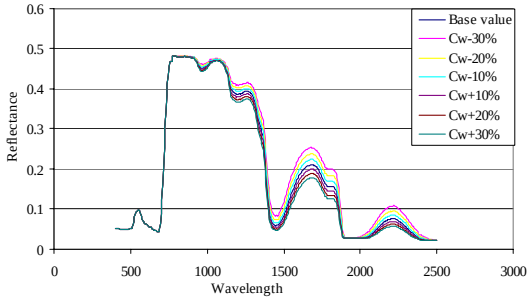

c) Water thickness (Cw)

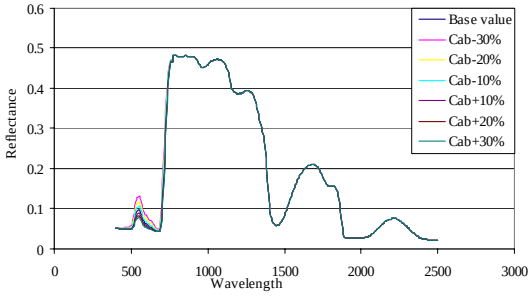

b) Chlorophyll (Cab)

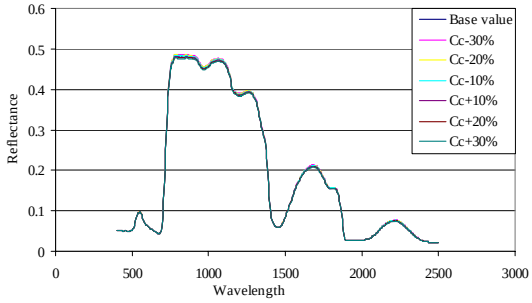

d) Cellulose + Lignin (Cc)

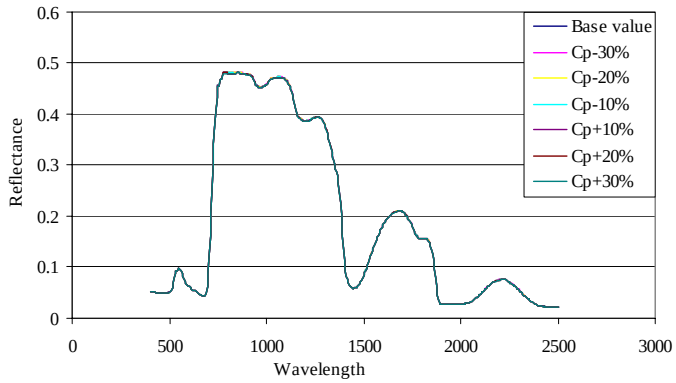

e) Protein (nitrogen, Cp)

Figure 5a-e. The diagrams from the sensitivity analysis of the PROSPECT-model.

The number of cell layers increases the reflectance almost throughout the whole spectra with peaks in green (0.5-0.6 μm), near infrared (0.72-1.3 μm) and middle infrared (1.3-3.0 μm). This is also demonstrated with the high values of the relative dimensionless index of sensibility (β, from Eq. 7) in table 7. An increasing amount of water increases the absorption in near infrared and middle infrared. Chlorophyll has an absorption feature in the visible part of the spectral with the biggest change in green light, while both protein and cellulose + lignin has minor impact on the reflectance data.

Table 7. The dimensionless index of sensibility for each parameter (base versus 30% change) in the wavelength boundary of each Landsat TM-channel.

Channel	N	Cab	Cw	Cp	Cc
TM1	0.172	0.063	0	0	0
TM2	0.878	0.495	0	0.004	0.008
TM3	0.453	0.196	0	0	0
TM4	0.461	0	0.005	0.007	0.031
TM5	0.784	0	0.548	0.006	0.040
TM7	1.208	0	0.816	0.014	0.074

6.4. Statistical results

The result of the correlation analysis is shown in Table 8, where the correlation coefficient (*r*) and eventually the *p*-value are presented. Overall, the correlation was quite low for most of the parameters and the only parameters showing relative high correlation

is reflectance data versus *SD* (*r* = 0.78 SD versus TM3) and the stands X-coordinate versus nitrogen (*r* = -0.88 Wc versus X-coordinate). Nitrogen had no significant correlation to any TM channel, the highest *r*-value is 0.49 to TM1.

Table 8. Correlation matrix between different stand parameter and the TM-channels, including the indices. On a few selected the p-value (significant) is presented in brackets.

Channel	LAI	SD	Wc (mg/g)	C (mg/g)
TM1	0.65	0.72 (0.020)	0.49	0.48
TM2	0.47	0.73 (0.018)	0.23	0.22
TM3	0.43	0.78 (0.008)	0.16	0.17
TM4	0.40	0.61	0.09	0.08
TM5	0.36	0.75 (0.012)	0.07	0.09
TM7	0.33	0.76 (0.011)	0.05	0.06
NDVI	-0.39	-0.76 (0.011)	-0.16	-0.17
SR	-0.19	-0.53	-0.04	-0.04
MSI	0.32	0.77 (0.009)	0.04	0.06
NDVI 4,7	-0.24	-0.71 (0.022)	0.03	0.02
X-coordinate	-0.58	0.04	-0.88 (0.001)	-0.87 (0.001)
Y-coordinate	0.05	-0.18	0.15	0.15

The stepwise regression between reflectance data and nitrogen concentration resulted in two TM-channels to be selected, TM1 and TM2 with an R^2-value of 0.72 (*wc* = 14.1 + 690 TM1 - 451 TM2). In Figure 6a, the weighted average of nitrogen is plotted against the fits and Figure 6b is showing the residuals versus fits. This is to detect if any anomalous data or trends exists. Optimal, the residuals in Figure 6b should be spread uniform over the plot, as homoscedasticity is required in the linear regression model (Zar, 1996).

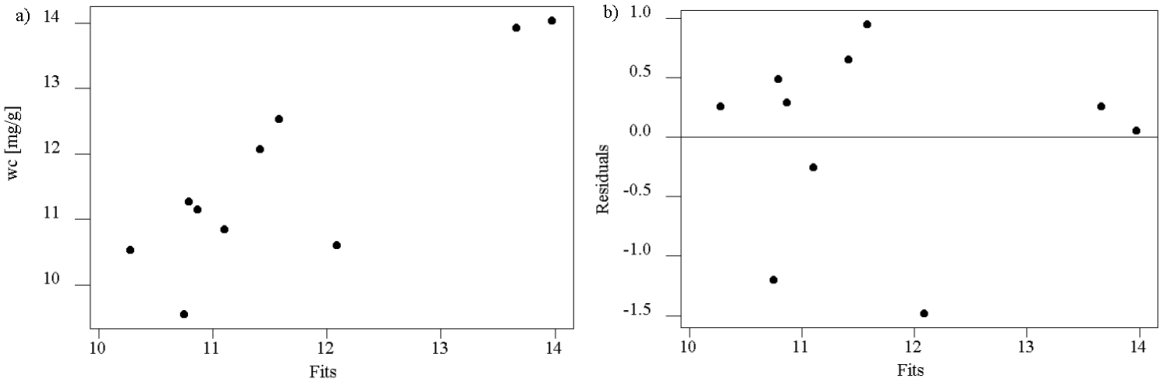

Figure 6. a) The relationship of wc versus fits and b) a plot of the residuals versus fits from the multiple regression between wc, TM1 and TM2.

In Figure 7, an example can be viewed of the plots between high- and low nitrogen status and the respective reflectance value of one TM-channel. No indication has been found on separability between these classes.

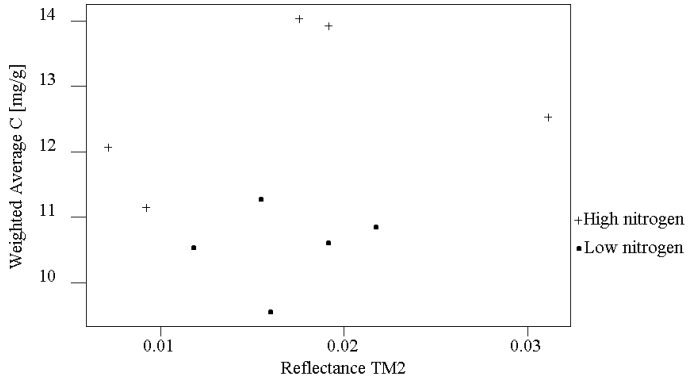

Figure 7. A plot for the classes 'high nitrogen' and 'low nitrogen' versus the respective reflectance values of Landsat channel TM2.

The regression for weighted average of nitrogen and the stands X-coordinate was significant (p = 0.001) with a R^2 = 0.77. The linear relationship can be view in Figure 8.

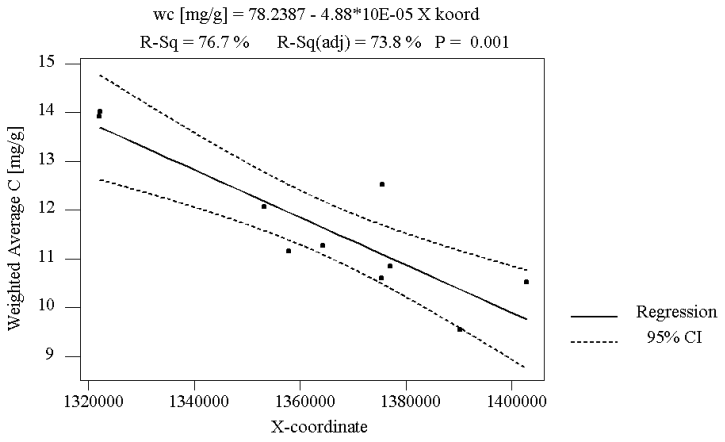

Figure 8. A linear relationship between the weighed average of nitrogen and the stands X-coordinate, R^2 = 0.77.

7. Discussion

The sensitivity analysis of the PROSPECT model indicated highest influence of both cell-structure and water thickness. Increasing the cell-structure creates a higher reflectance in the whole spectrum whilst higher water thickness absorbs the incoming radiation in the higher wavelength (near- and mid-infrared). Chlorophyll has an absorption feature only in the visible part of the spectrum, with the highest sensitivity in green. This may introduce a problem if the model is used in inverted mode (input data are reflectance and a set of parameters, chlorophyll is the concentration to retrieve, chapter 3.2) as chlorophyll has an 'absorptive' response in green and the cell-structure has a 'reflective' response. Imagine a small additive error (1.7 instead of 1.6) in the parameter cell-structure, this would mean an increase of reflectance in green light that would also correspond to a lower concentration of chlorophyll. Hence, it is possible that the opposite response of these two parameters could counteract each other, creating an uncertainly of the modeled value, if the input data has errors. However, changing the cell-structure up to +30% from the 'normal' value may not be a representative change. Jacquemoud *et al*. (1996) reported a structure parameter that ranged from 1.5-2.5 for dicotyledons in vegetation grown in a greenhouse, but the range does not seem to apply for vegetation grown outside under natural conditions. Lignin+cellulose and protein showed only minor absorption features in the simulated spectra. This is a known feature of the creator of the model (Jacquemoud *et al.*, 1996) and is explained by the low percentage of the constituents in the leaves, for example only 1-5 % of the leaves mass is related to nitrogen compounds. In addition, in inverted mode, the water absorption could eventually mask the absorption feature of lignin+cellulose and protein in the middle infrared, as water absorption is a lot stronger.

The different channels of Landsat TM had no correlation with nitrogen with the eventual exception of TM1 (non-significant). This indicates that the Landsat TM-channels are not able to detect the different absorption features of nitrogen. In contrast to this, the multiple regression with TM1 and TM2 predicting nitrogen showed a promising result. However, the correlation found in the regression can possible be related to chlorophyll contents

instead of nitrogen, as they both are reported to be correlated and covariable (Jacquemoud *et al*., 1996; Curran & Kupiec, 1995). This means the regression would show the indirect relationship of nitrogen content through chlorophyll's absorption feature in the visible part of the spectrum. It is doubtful that the connections between nitrogen and chlorophyll are strong enough to stand as a medium for estimation of nitrogen concentration through their combined absorption features with the coarse spectral resolution of Landsat TM. Due to the low number of observations (n = 10) the statistics should be interpreted cautiously and the results is far from final. A more accurate study with more observations would lead to a better result. This to better distinguish whether or not, and to what possible extent, the reflectance values of Landsat TM contains information of the nitrogen in the needles.

The high correlation of the X-coordinate and nitrogen amount suggests that an 'outside' factor influences the nitrogen level in the needles. That the gradient from west to east exists (higher in west) is shown with the regression and there may be various causes for this. However, one logical explanation to this phenomena is a higher deposition of nitrogen on the west side of Scania, and the nitrogen in the needles are likely to have a connection to the nitrogen available in the ground.

7.1 Sources of error

The following sources of errors have been identified and could possible have influenced the results of this study:

1) Errors in the fieldwork and LAI-calculation

- The method used to calculate LAI is using a regression with a known confidence level, Nilson *et al*. (1999) reported an error of approximately 20 % in the LAI calculation. In addition, the conversion coefficient is from the same study, and may not be representative for the stands used in this study.
- Other biochemical constituents should have been measured, as water thickness and chlorophyll.

- Nitrogen concentrations were measured from all needles of the five trees in each stand, hence only reflect a mean value. It would have been desired to have each trees' nitrogen concentration measured separately, thus creating a mean value and a standard deviation from each stand.

2) Errors in the sensitivity analysis of the PROSPECT model

- The different parameters are varied with the same scale (-30 % to +30 %) with the assumption that this would be representative to a natural environment. However, this may not be true.
- The correlation / covariance between the parameters are not taken into consideration. Hence, when increasing nitrogen, chlorophyll would also increase that would create a different outcome of the simulated spectra.

3) Errors in the statistical analysis

- The different analysis may only be interpreted as 'an indication' as the number of measurements is a bit low.

The biggest source of error in this study is the low number of stands investigated. It creates an obscurity in the statistical analysis and it would be desired to have at least double the amount of measurements to be able to interpret the result correctly.

8. Conclusion

The PROSPECT model showed a minor sensitivity to protein/nitrogen concentrations, thus using the model to predict nitrogen amounts in needles is doubtful. Hence, it is unlikely that other models, using PROSPECT to explain the leaf optical properties, are able to predict nitrogen with a reasonable precision. The use of Landsat TM as source of reflectance values for these types of studies is still not certain. However, an indication can be seen that the coarse spectral resolution of the sensor may not provide the desired information. Still, nitrogen has absorption features throughout the spectra, but only in narrow parts. Thus, for further analysis, hyper-spectral data is recommended. The W-E nitrogen gradient found in this study cannot be observed in the remotely sensed data, but still it indicates that there may be other ways to simplify the collection of nitrogen amounts in needles, for example through ground chemistry measurements.

9. References

Balsberg-Phålson A-M., 1990. Handledning i Kemiska Metoder vid Växtekologiska Arbeten. Meddelande från Växtekologiska institutionen, nummer 52, Lunds universitet, 58pp.

Baret F., 1995. Use of Spectral Reflectance Variation to Retrieve Canopy Biophysical Characteristics, in Advances in Environmental Remote Sensing (Danson F. M., & Plummer S. E., Ed.). John Wiley & Sons.

Berk A., Bernstein L. S. & Robertson D. C., 1989. MODTRAN: A Moderate Resolution Model for LOWTRAN 7. Hanscom Air Force Base, MA: Air Force Geophysics Laboratory, 38pp.

Campbell B. J., 1996. Introduction to Remote Sensing (Second Edition). Taylor & Francis, London.

Curran P. J., Dungan J. L. & Peterson D. L., 2001. Estimating the foliar biochemical concentration of leaves with reflectance spectrometry: Testing the Kokaly and Clark methodologies. *Remote Sens. Environ.*, 76:349-359.

Curran P.J & Kupiec J. A., 1995. Imaging Spectrometry: A New Tool for Ecology, in Advances in Environmental Remote Sensing (Danson F. M., & Plummer S. E., Ed.). John Wiley & Sons.

Danson F. M., 1995. Developments in the Remote Sensing of Forest Canopy Structure, in Advances in Environmental Remote Sensing (Danson F. M., & Plummer S. E., Ed.). John Wiley & Sons.

Dawson T. P., Curran P. J., North P. R. J., and Plummer S. E., 1999. The Propagation of Foliar Biochemical Absorption in Forest Canopy Reflectance: A Theoretical Analysis. *Remote Sens. Environ.*, 67:147-159.

Dawson T. P., Curran P. J. & Plummer S. E., 1998. LIBERTY – Modelling the Effects of Leaf Biochemical Concentration of Reflectance Spectra. *Remote Sens. Environ.*, 65:50-60.

Endo T., Okuda T., Tamura M., & Yasuoka Y., 2000. Estimation of Photosynthetic Rate of Plant from Hyper-spectral Remote Sensing of Biochemical Content. Asian Conference on Remote Sensing (ARCS), Hyperspectral & Data Acquisition Systems, December 4-8, 2000, Taipei, Taiwan.

Friend A. D., 1995. PGEN: An integrated model of leaf photosynthesis, transpiration and conductance. *Ecological Modelling*. 77(2-3):233-256.

GCPworks 1997. GCPworks – Reference Manual (Version 6.2). PCI, Ontario, Canada.

Goel N. S., 1989. Inversion of Canopy Reflectance Models for Estimation of Biophysical Parameters from Reflectance Data, in Theory and Applications of Optical Remote Sensing (Asrar G., Ed.). John Wiley & Sons.

Goetz A. F. H., Gao B. C., Wessman C. A. & Bowman W. D., 1990. Estimation of biochemical constituents from fresh, green leaves by spectrum matching techniques, in Proc, 10th Geosci. And Remote Sens. Symp. (IGARSS'90), University of Maryland (MD), 20-24 May 1990, 971-974.

Hosgood B., Jacquemoud S., Andreoli G., Verdebout J., Pedrini G., & Schmuck G., 1995. Leaf Optical Properties Experiment 93 (LOPEX93). Joint Research Center / Institute for Remote Sensing Applications, Ispra, Italy.

Jacquemoud S., & Ustin S. L., 2001. Leaf Optical Properties: A State Of The Art. Pages 223-232 in 8th Int. Symp. Physical Measurements & Signatures in Remote Sensing, Aussois, France.

Jacquemoud S., Ustin S. L., Verdebout J., Schmuck G., Andreoli G., & Hosgood B., 1996. Estimating leaf biochemistry using the PROSPECT leaf optical properties model. *Remote Sens. of Environ.*, 56:194-202.

Jacquemoud S., 1993. Inversion of the PROSPECT + SAIL Canopy Reflectance Model from AVIRIS Equivalent Spectra: Theoretical Study. *Remote Sens. Environ.*, 44:281-292.

Jacquemoud S., & Baret F., 1990. PROSPECT: A model of Leaf Optical Properties Spectra. *Remote Sens. Environ.*, 34:75-91.

Jordan C. F., 1969. Derivation of leaf area index from quality of light on the forest floor. *Ecology*. 50:663-666.

Kaufman Y. J., 1989. The atmospheric Effect on Remote Sensing and its Correction, in Theory and Applications of Optical Remote Sensing (Asrar G., Ed.). John Wiley & Sons.

Kniezys F. X., Shettle E. P., Abreu, L. W., Chetwynd J H., Anderson G. P., Gallery W. O., Selby J. E. A. & Clough S. A., 1988. Users Guide to LOWTRAN 7. Hanscom Air Force Base, MA: Air Force Geophysics Laboratory, 137pp.

Kokaly R. F., and Clark R. N., 1999. Spectroscopic Determination of Leaf Biochemistry Using Band-Depth Analysis of Absorption Features and Stepwise Multiple Linear Regression. *Remote Sens. Environ.*, 67:267-287.

Kuusk A., & Nilson T., 2000. A Directional Multispectral Forest Reflectance Model. *Remote Sens. Environ.,* 72:244-252.

Kuusk A., 1994. A Multispectral Canopy Reflectance Model. *Remote Sens. Environ.,* 50:75-82.

Lillesand T. M., & Kiefer R. W., 2000. Remote Sensing and Image Interpretation (Fourth Edition). John Wiley & Sons.

Nemani R., Pierce L., Running S., & Band L., 1993. Forest ecosystem processes at the watershed scale: sensitivity to remotely-sensed leaf area index estimates. *Int. J. Remote Sens.,* 14:2519-2534.

Nilson T., Anniste J., Lang M., & Praks J., 1999. Determination of needle area indices of coniferous forest in the NOPEX region by ground-based optical measurements and satellite images. *Agricultural and Forest Meteorology,* 98-99:449-462.

Markham B.L., & Barker J.L., 1986. Landsat MSS and TM post-calibration dynamic ranges. Exoatmospheric reflectances and at-satellite temperatures. Landsat Technical Notes, no. 1. NASA/Goddard Space Flight Center, Greenbelt, MD.

Marklund L. G., 1988. Biomass functions for pine, spruce and birch in Sweden. Swedish University of Agricultural Science, Department of Forest Survey, Report 45, Umeå, 78pp.

O'Neill A. L., Kupiec J. A., & Curran P. J., 2002. Biochemical and reflectance variation throughout a Sitka spruce canopy. *Remote Sens. Environ.,* 80:134-142.

Rouse J. W., Haas R. H., Schell J. A., & Deering D. W., 1973. Monitoring vegetation systems in the great plains with ERTS. Third ERTS symposium, NASA SP-351. December 10-14, I:309-317. Washington D. C.

Serrano L., Peñuelas J., & Urstin S. L., 2002. Remote sensing of nitrogen and lignin in Mediterranean vegetation from AVIRIS data: Decomposing biochemical from structural signals. *Remote Sens. Environ.,* 81:355-364.

Skånes Samrådsgrupp mot Skogsskador, 1986. Fasta skogsprovytor i Skåne – för uppföljning av skogsskador. Rapport 1/86. Länstyrelsen i Kristianstad län, Sverige.

Skånes Samrådsgrupp mot Skogsskador, 1987. Flygbildsbaserad inventering av skogsskador på gran och tall i Skåne 1986. Rapport 4/87. Länstyrelsen i Kristianstad län, Sverige.

Skånes Samrådsgrupp mot Skogsskador, 1992a. Barrkemi och barrstrukturer på skogsprovytor i Skåne 1990. Rapport 11/92. Länstyrelsen i Kristianstad län, Sverige.

Skånes Samrådsgrupp mot Skogsskador, 1992b. Fasta skogsprovytor i Skåne – Dataöversikter 1984/85 – 1989/90. Rapport 12/92. Länstyrelsen i Kristianstad län, Sverige.

Skånes Samrådsgrupp mot Skogsskador, 1993. Tillväxt och barrförlust hos gran och tall i Skåne 1985-1990 – Relation till markförsuring, näringsämnen och beståndsålder. Rapport 15/93. Länstyrelsen i Kristianstad län, Sverige.

Skånes Samrådsgrupp mot Skogsskador, 1997. Barrkemi på Skånska gran- och tallprovytor 1994 – relationer till markkemi och tillväxt. Rapport 17/96. Länstyrelsen i Kristianstad län, Sverige.

Vermote E. F., Tanré D., Deuzé J. L., Herman M., & Morcrette J. J., 1997a. 6S User Guide Version 2, Second Simulation of the Satellite Signal in the Solar Spectrum (6S). University of Maryland/Laboratoire d'Optique Atmospherique.

Vermote E. F., Tanré D., Deuzé J. L., Herman M., & Morcrette J. J., 1997b. Second Simulation of the Satellite Signal in the Solar Spectrum, 6S: An Overview. *Ieee Transactions on Geoscience and Remote Sensing*, vol. 35, no. 3, 675-686.

Vogelmann J.E., 1990. Comparison between two vegetation indices for measuring different types of forest damage in the north-eastern United States. *Int. J. Remote Sens.*, 11:2281-2297.

Zar J. H., 1996. Biostatistical analysis (Third edition). Prentice Hall International Editions, New Jersey.

9.1 Internet references

ESA, 2002. Earth Observation Earthnet Online
http://earth.esa.int/0xc1cce41c_0x0000069c (020812).

10. Appendixes

Appendix 1. An example of input-file to 6S- model.

```
7                                 (LANDSAT)
4 7 9.4221 13.4507923 55.9131279 (month, day, hh.ddd, long., lat. 2000 04 07 kl:)
8                                 (User's model)
0.684 0.34                        (H2O, O3)
2                                 (Aerosol model, maritime)
0                                 (NEXT VALUE IS THE AERO. OPT. THICK. @550nm)
0.089145712                       (AERO. OPT. THICK. @550nm)
-0.1                              (TARGET AT 0.1 km)
-1000                             (REMOTE SENSING SENSOR HEIGHT - DEFAULT VALUE)
25                                (LANDSAT TM 5, BAND 1 = 25, BAND 7 = 30)
0                                 (GROUND TYPE,I.E. 0 = homogeneous)
0                                 (DIRECTIONNAL EFFECTS)
1                                 (vegetated target surface)
-0.0835                           (input at satellite reflectance)
```

Appendix 2. An example of an output-file from 6S-model.

```
****************************** 6s version 4.1 ****************************** *
*                                                                             *
*                       geometrical conditions identity                       *
*                       -------------------------------                       *
*                       t.m.     observation                                  *
*                 month:  4 day :   7 universal time:  9.42 (hh.dd)           *
*                latitude:   55.91 deg        longitude:   13.45 deg          *
*   solar zenith angle:   53.08 deg  solar azimuthal angle:      147.33 deg   *
*   view zenith angle:     0.00 deg  view azimuthal angle:         0.00 deg   *
*   scattering angle:    126.92 deg  azimuthal angle difference: 147.33 deg   *
*                                                                             *
*                       atmospheric model description                         *
*                       -----------------------------                         *
*           atmospheric model identity :                                      *
*             user defined water content : uh2o= 0.684 g/cm2                  *
*             user defined ozone content : uo3 = 0.340 cm-atm                 *
*           aerosols type identity :                                          *
*                      Maritime aerosols model                                *
*           optical condition identity :                                      *
*                visibility : 73.51 km  opt. thick. 550nm : 0.0891            *
*                                                                             *
*                       spectral condition                                    *
*                       ------------------                                    *
*            tm  1                                                            *
*               value of filter function :                                    *
*                wl inf= 0.430 mic   wl sup= 0.560 mic                        *
*                                                                             *
*                       target type                                           *
*                       -----------                                           *
*           homogeneous ground                                                *
*             spectral vegetation ground reflectance 0.104                    *
*                                                                             *
*                       target elevation description                          *
*                       ----------------------------                          *
*           ground pressure  [mb] 1000.93                                     *
*           ground altitude  [km] 0.100                                       *
*                gaseous content at target level:                             *
*                uh2o= 0.684 g/cm2        uo3= 0.340 cm-atm                  *
*                                                                             *
*                        atmospheric correction activated                     *
*                        --------------------------------                     *
*           input apparent reflectance :  0.083                               *
*                                                                             *
******************************************************************************



******************************************************************************
*                                                                             *
*                         integrated values of  :                             *
*                         -----------------------                             *
*       apparent reflectance  0.1565    appar. rad.(w/m2/sr/mic)     58.516   *
*                    total gaseous transmittance  0.982                       *
*                                                                             *
******************************************************************************
*                                                                             *
*                         coupling aerosol -wv  :                             *
*                         -----------------------                             *
*           wv above aerosol :   0.157     wv mixed with aerosol :   0.157    *
*                        wv under aerosol :   0.157                           *
*                                                                             *
*                         int. normalized  values  of  :                      *
*                         ------------------------------                      *
*                       % of irradiance at ground level                       *
*     % of direct  irr.    % of diffuse irr.    % of enviro. irr              *
*                0.750               0.236               0.015                *
*                       reflectance at satellite level                        *
*     atm. intrin. ref.   background  ref.  pixel  reflectance                *
```

```
*               0.075               0.012               0.070                *
*                                                                            *
*                          int. absolute values of                           *
*                          -----------------------                           *
*                       irr. at ground level (w/m2/mic)                      *
*     direct solar irr.    atm. diffuse irr.    environment  irr              *
*             759.657             238.472             14.920                 *
*                       rad at satel. level (w/m2/sr/mic)                    *
*     atm. intrin. rad.    background  rad.    pixel  radiance               *
*              27.864               4.613             26.039                 *
*                                                                            *
*                                                                            *
*          int. funct filter (in mic)              int. sol. spect (in w/m2) *
*             0.0604850                                 118.245             *
*                                                                            *
******************************************************************************
```

```
******************************************************************************
*                                                                            *
*                           integrated values of  :                          *
*                           -------------------                              *
*                                                                            *
*                              downward        upward          total         *
*      global gas. trans. :    0.98843        0.99302        0.98157         *
*      water   "     "    :    1.00000        1.00000        1.00000         *
*      ozone   "     "    :    0.98843        0.99302        0.98157         *
*      co2     "     "    :    1.00000        1.00000        1.00000         *
*      oxyg    "     "    :    1.00000        1.00000        1.00000         *
*      no2     "     "    :    1.00000        1.00000        1.00000         *
*      ch4     "     "    :    1.00000        1.00000        1.00000         *
*      co      "     "    :    1.00000        1.00000        1.00000         *
*                                                                            *
*                                                                            *
*      rayl.  sca. trans. :    0.87788        0.92245        0.80980         *
*      aeros. sca.   "    :    0.97912        0.99198        0.97126         *
*      total  sca.   "    :    0.86010        0.91425        0.78634         *
*                                                                            *
*                                                                            *
*                                                                            *
*                              rayleigh       aerosols         total         *
*                                                                            *
*      spherical albedo   :    0.12607        0.02723        0.14347         *
*      optical depth total:    0.16317        0.09195        0.25512         *
*      optical depth plane:    0.16317        0.09195        0.25512         *
*      reflectance        :    0.06982        0.00423        0.07581         *
*      phase function     :    1.01975        0.09831        0.68764         *
*      sing. scat. albedo :    1.00000        0.98957        0.99624         *
*                                                                            *
*                                                                            *
******************************************************************************
******************************************************************************
```

```
******************************************************************************
*                       atmospheric correction result                        *
*                       -----------------------------                        *
*       input apparent reflectance            :    0.083                     *
*       measured radiance [w/m2/sr/mic]       :   31.211                     *
*       atmospherically corrected reflectance :    0.012                     *
*       coefficients xa xb xc                 :  0.00347  0.09821  0.14347   *
*       y=xa*(measured radiance)-xb;  acr=y/(1.+xc*y)                        *
******************************************************************************
```

Lunds Universitets Naturgeografiska institution. Seminarieuppsatser. Uppsatserna finns tillgängliga på Naturgeografiska institutionens bibliotek, Sölvegatan 13, 223 62 LUND.

The reports are available at the Geo-Library, Department of Physical Geography, University of Lund, Sölvegatan 13, S-223 62 Lund, Sweden.

1. Pilesjö, P. (1985): Metoder för morfometrisk analys av kustområden.
2. Ahlström, K. & Bergman, A. (1986): Kartering av erosionskänsliga områden i Ringsjöbygden.
3. Huseid, A. (1986): Stormfällning och dess orsakssamband, Söderåsen, Skåne.
4. Sandstedt, P. & Wällstedt, B. (1986): Krankesjön under ytan - en naturgeografisk beskrivning.
5. Johansson, K. (1986): En lokalklimatisk temperaturstudie på Kungsmarken, öster om Lund.
6. Estgren, C. (1987): Isälvsstråket Djurfälla-Flädermo, norr om Motala.
7. Lindgren, E. & Runnström, M. (1987): En objektiv metod för att bestämma läplanteringars läverkan.
8. Hansson, R. (1987): Studie av frekvensstyrd filtringsmetod för att segmentera satellitbilder, med försök på Landsat TM-data över ett skogsområde i S. Norrland.
9. Matthiesen, N. & Snäll, M. (1988): Temperatur och himmelsexponering i gator: Resultat av mätningar i Malmö.
10A. Nilsson, S. (1988): Veberöd. En beskrivning av samhällets och bygdens utbyggnad och utveckling från början av 1800-talet till vår tid.
10B. Nilson, G., 1988: Isförhållande i södra Öresund.
11. Tunving, E. (1989): Översvämning i Murciaprovinsen, sydöstra Spanien, november 1987.
12. Glave, S. (1989): Termiska studier i Malmö med värmebilder och konventionell mätutrustning.
13. Mjölbo, Y. (1989): Landskapsförändringen - hur skall den övervakas?
14. Finnander, M-L. (1989): Vädrets betydelse för snöavsmältningen i Tarfaladalen.
15. Ardö, J. (1989): Samband mellan Landsat TM-data och skogliga beståndsdata på avdelningsnivå.
16. Mikaelsson, E. (1989): Byskeälvens dalgång inom Västerbottens län. Geomorfologisk karta, beskrivning och naturvärdesbedömning.
17. Nhilen, C. (1990): Bilavgaser i gatumiljö och deras beroende av vädret. Litteraturstudier och mätning med DOAS vid motortrafikled i Umeå.
18. Brasjö, C. (1990): Geometrisk korrektion av NOAA AVHRR-data.
19. Erlandsson, R. (1991): Vägbanetemperaturer i Lund.
20. Arheimer, B. (1991): Näringsläckage från åkermark inom Brååns dräneringsområde. Lokalisering och åtgärdsförslag.
21. Andersson, G. (1991): En studie av transversalmoräner i västra Småland.
22A. Skillius, Å., (1991): Water havesting in Bakul, Senegal.
22B. Persson, P. (1991): Satellitdata för övervakning av höstsådda rapsfält i Skåne.
23. Michelson, D. (1991): Land Use Mapping of theThat Luang - Salakham Wetland, Lao PDR, Using Landsat TM-Data.

24. Malmberg, U. (1991): En jämförelse mellan SPOT- och Landsatdata för vegetations-klassning i Småland.
25. Mossberg, M. & Pettersson, G. (1991): A Study of Infiltration Capacity in a Semiarid Environment, Mberengwa District, Zimbabwe.
26. Theander, T. (1992): Avfallsupplag i Malmöhus län. Dränering och miljö-påverkan.
27. Osaengius, S. (1992): Stranderosion vid Löderups strandbad.
28. Olsson, K. (1992): Sea Ice Dynamics in Time and Space. Based on upward looking sonar, satellite images and a time series of digital ice charts.
29. Larsson, K. (1993): Gully Erosion from Road Drainage in the Kenyan Highlands. A Study of Aerial Photo Interpreted Factors.
30. Richardson, C. (1993): Nischbildningsprocesser - en fältstudie vid Passglaciären, Kebnekaise.
31. Martinsson, L. (1994): Detection of Forest Change in Sumava Mountains, Czech Republic Using Remotely Sensed Data.
32. Klintenberg, P. (1995): The Vegetation Distribution in the Kärkevagge Valley.
33. Hese, S. (1995): Forest Damage Assessment in the Black Triangle area using Landsat TM, MSS and Forest Inventory data.
34. Josefsson, T. och Mårtensson, I. (1995). A vegetation map and a Digital Elevation Model over the Kapp Linné area, Svalbard -with analyses of the vertical and horizontal distribution of the vegetation.
35. Brogaard, S och Falkenström, H. (1995). Assessing salinization, sand encroach-ment and expanding urban areas in the Nile Valley using Landsat MSS data.
36. Krantz, M. (1996): GIS som hjälpmedel vid växtskyddsrådgivning.
37. Lindegård, P. (1996). Vinterklimat och vårbakslag. Lufttemperatur och kåd-flödessjuka hos gran i södra Sverige.
38. Bremborg, P. (1996). Desertification mapping of Horqin Sandy Land, Inner Mongolia, by means of remote sensing.
39. Hellberg, J. (1996). Förändringsstudie av jordbrukslandskapet på Söderslätt 1938-1985.
40. Achberger, C. (1996): Quality and representability of mobile measurements for local climatological research.
41. Olsson, M. (1996): Extrema lufttryck i Europa och Skandinavien 1881-1995.
42. Sundberg, D. (1997): En GIS-tillämpad studie av vattenerosion i sydsvensk jord-bruksmark.
43. Liljeberg, M. (1997): Klassning och statistisk separabilitetsanalys av marktäck-ningsklasser i Halland, analys av multivariata data Landsat TM och ERS-1 SAR.
44. Roos, E. (1997): Temperature Variations and Landscape Heterogeneity in two Swedish Agricultural Areas. An application of mobile measurements.
45. Arvidsson, P. (1997): Regional fördelning av skogsskador i förhållande till mängd SO_2 under vegetationsperioden i norra Tjeckien.
46. Akselsson, C. (1997): Kritisk belastning av aciditet för skogsmark i norra Tjeckien.
47. Carlsson, G. (1997): Turbulens och supraglacial meandring.
48. Jönsson, C. (1998): Multitemporala vegetationsstudier i nordöstra Kenya med AVHRR NDVI

49. Kolmert, S. (1998): Evaluation of a conceptual semi-distributed hydrological model – A case study of Hörbyån.
50. Persson, A. (1998): Kartering av markanvändning med meteorologisk satellitdata för förbättring av en atmosfärisk spridningsmodell.
51. Andersson, U. och Nilsson, D. (1998): Distributed hydrological modelling in a GIS perspective – an evaluation of the MIKE SHE model.
52. Andersson, K. och Carlstedt, J. (1998): Different GIS and remote sensing techniques for detection of changes in vegetation cover - A study in the Nam Ngum and Nam Lik catchment areas in the Lao PDR.
53. Andersson, J., (1999): Användning av global satllitdata för uppskattning av spannmålsproduktion i västafrikanska Sahel.
54. Flodmark, A.E., (1999): Urban Geographic Information Systems, The City of Berkeley Pilot GIS
55A. Lyborg, Jessic & Thurfell, Lilian (1999): Forest damage, water flow and digital elevation models: a case study of the Krkonose National Park, Czech Republic.
55B. Tagesson, I., och Wramneby, A., (1999): Kväveläckage inom Tolångaåns dräneringsområde – modellering och åtgärdssimulering.
56. Almkvist, E., (1999): Högfrekventa tryckvariationer under de senaste århundradena.
57. Alstorp, P., och Johansson, T., (1999): Översiktlig buller- och luftföroreningsinventering i Burlövs Kommun år 1994 med hjälp av geografiska informationssystem – möjligheter och begränsningar.
58. Mattsson, F., (1999): Analys av molnklotter med IRST-data inom det termala infraröda våglängdsområdet
59. Hallgren, L., och Johansson, A., (1999): Analysing land cover changes in the Caprivi Strip, Namibia, using Landsat TM and Spot XS imagery.
60. Granhäll, T., (1999): Aerosolers dygnsvariationer och långväga transporter.
61. Kjellander, C., (1999): Variations in the energy budget above growing wheat and barley, Ilstorp 1998 - a gradient-profile approach
62. Moskvitina, M., (1999): GIS as a Tool for Environmental Impact Assessment - A case study of EIA implementation for the road building project in Strömstad, Sweden
63. Eriksson, H., (1999): Undersökning av sambandet mellan strålningstemperatur och NDVI i Sahel.
64. Elmqvist, B., Lundström, J., (2000): The utility of NOAA AVHRR data for vegetation studies in semi-arid regions.
65. Wickberg, J., (2000): GIS och statistik vid dräneringsområdesvis kväveläckagebeskrivning i Halland.
66. Johansson, M., (2000): Climate conditions required for re-glaciation of cirques in Rassepautasjtjåkka massif, northern Sweden.
67. Asserup, P., Eklöf, M., (2000): Estimation of the soil moisture distribution in the Tamne River Basin, Upper East Region, Ghana.
68. Thern, J., (2000): Markvattenhalt och temperatur i sandig jordbruksmark vid Ilstorp, centrala Skåne: en mätnings- och modelleringsstudie.
69. Andersson, C., Lagerström, M., (2000): Nitrogen leakage from different land use

types - a comparison between the watersheds of Graisupis and Vardas, Lithuania.
70. Svensson, M., (2000): Miljökonsekvensbeskrivning med stöd av Geografiska Informationssystem (GIS) – Bullerstudie kring Malmö-Sturup Flygplats.
71. Hyltén, H.A., Uggla, E., (2000): Rule.Based Land Cover Classification and Erosion Risk Assessment of the Krkonoše National Park, Czech Republic.
72. Cronquist, L., Elg, S., (2000): The usefulness of coarse resolution satellite sensor data for identification of biomes in Kenya.
73. Rasmusson, A-K., (2000): En studie av landskapsindex för kvantifiering av rumsliga landskapsmönster.
74. Olofsson, P., Stenström, R., (2000): Estimation of leaf area index in southern Sweden with optimal modelling and Landsat 7 ETM+Scene.
75. Uggla, H., (2000): En analys av nattliga koldioxidflöden i en boreal barrskog avseende spatial och temporal variation.
76. Andersson, E., Andersson, S., (2000): Modellering och uppmätta kväveflöden i energiskog som bevattnas med avloppsvatten.
77. Dawidson, E., Nilsson, C., (2000): Soil Organic Carbon in Upper East Region, Ghana - Measurements and Modelling.
78. Bengtsson, M., (2000): Vattensänkningar - en analys av orsaker och effekter.
79. Ullman, M., (2001): El Niño Southern Oscillation och dess atmosfäriska fjärrpåverkan.
80. Andersson, A., (2001): The wind climate of northwestern Europe in SWECLIM regional climate scenarios.
81. Lalloo, D., (2001): Geografiska informationssystem för studier av polyaromatiska kolväten (PAH) – Undersökning av djupvariation i BO01-området, Västra hamnen, Malmö, samt utveckling av en matematisk formel för beräkning av PAH-koncentrationer från ett kontinuerligt utsläpp.
82. Almqvist, J., Fergéus, J., (2001): GIS-implementation in Sri Lanka.
Part 1: GIS-applications in Hambantota district Sri Lanka : a case study.
Part 2: GIS in socio-economic planning : a case study.
83. Berntsson, A., (2001): Modellering av reflektans från ett sockerbetsbestånd med hjälp av en strålningsmodell.
84. Umegård, J., (2001): Arctic aerosol and long-range transport.
85. Rosenberg, R., (2002): Tetratermmodellering och regressionsanalyser mellan topografi, tetraterm och tillväxt hos sitkagran och lärk – en studie i norra Island.
86. Håkansson, J., Kjörling, A., (2002):
87. Arvidsson, H., (2002): Coastal parallel sediment transport on the SE Australian inner shelf – A study of barrier morphodynamics.
88. Bemark, M., (2002): Köphultssjöns tillstånd och omgivningens påverkan.
89. Dahlberg, I., (2002): Rödlistade kärlväxter i Göteborgs innerstad – temporal och rumslig analys av rödlistade kärlväxter i Göteborgs artdataarkiv, ADA.
90. Poussart, J-N., (2002): Verification of Soil Carbon Sequestration - Uncertainties of Assessment Methods.
91. Jakubaschk, C., (2002): Acacia senegal, Soil Organic Carbon and Nitrogen Contents: A Study in North Kordofan, Sudan.
92. Lindquist, S., (2002): Investigating the use of Landsat TM for mapping leaf nitrogen of Norway spruce.